Linear Viscoelasticity of Polyelectrolyte Complex Coacervates

Supporting Information

Evan Spruijt,* Martien A. Cohen Stuart, and Jasper van der Gucht

Laboratory of Physical Chemistry and Colloid Science, Wageningen University, Dreijenplein 6, 6703 HB Wageningen, The Netherlands

Fraction of charged groups on PDMAEMA and PAA

Figure 1 shows a pH titration of PAA_{20}, starting from a fully protonated form, at different salt concentrations. We approximate the deprotonation equilibrium of PAA using a single effective pK_a, which is taken as the pH halfway of the equivalence point. The effective pK_a is about 5.5 at 0.10 M salt, almost independent of chain length, but decreasing with increasing salt concentration to about 5.0 at 1.0 M salt.

For PDMAEMA we find a similar behavior, but now protonation occurs as the pH is lowered. For PDMAEMA we find an effective pK_b of 7.5 at 0.10 M salt, increasing with increasing salt concentration to about 7.9 at 1.0 M salt.

Figure 2 shows the calculated degree of ionization as a function of pH for PAA of two different chain lengths and PDMAEMA of one single chain length, all at two different salt concentrations. The degree of ionization is calculated according to

$$\alpha_- = \frac{10^{\mathrm{pH}-\mathrm{p}K_a}}{1+10^{\mathrm{pH}-\mathrm{p}K_a}} \tag{1}$$

$$\alpha_+ = \frac{10^{\mathrm{p}K_b-\mathrm{pH}}}{1+10^{\mathrm{p}K_b-\mathrm{pH}}}$$

All our complex coacervates are prepared with PAA and PDMAEMA stock solutions at pH 6.5, where both polyelectrolytes have equal charge densities at salt concentrations between 0.10 M and 1.0 M ($\alpha_+ = \alpha_- = 0.95$).

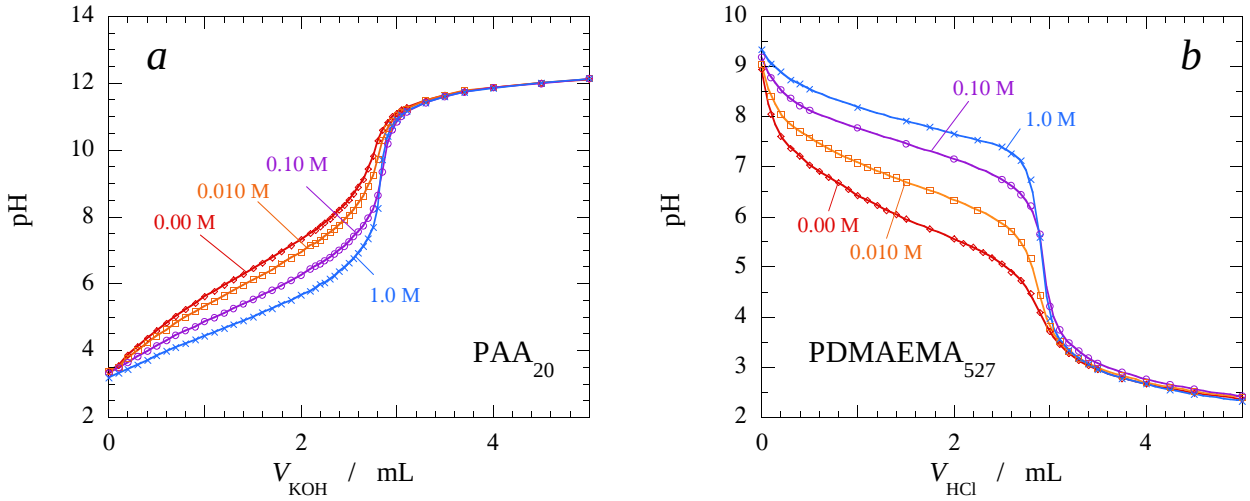

Figure 1: (a) pH titration of a 250 mL 1.0 g/L solution of PAA_{20}, acidic form, with a 1.0 M KOH solution, at four concentrations of KCl. (b) pH titration of a 250 mL 2.0 g/L solution of $PDMAEMA_{527}$, basic form, with a 1.0 M HCl solution, at four concentrations of KCl. 0.00 M indicates no added salt.

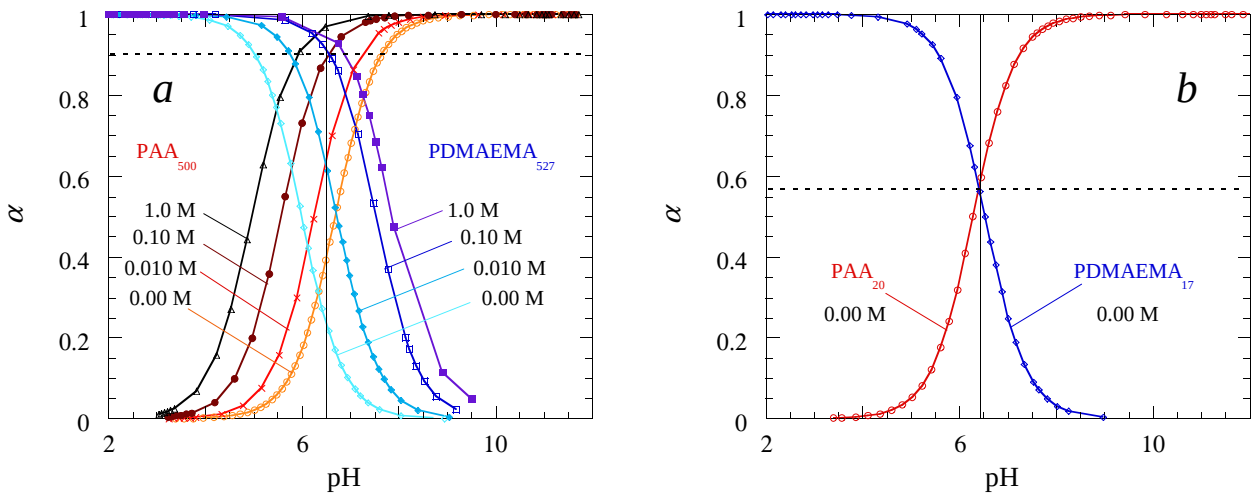

Figure 2: (a) Degree of ionization, α, for PAA_{500} and $PDMAEMA_{527}$ as a function of pH at four concentrations of KCl. 0.00 M indicates no added salt. (b) Degree of ionization, α, for PAA_{20} and $PDMAEMA_{17}$ as a function of pH with no added salt.

pH changes upon complexation

Both PAA and PDMAEMA stock solutions are prepared at pH = 6.5 $\pm$ 0.2. We have measured the change in pH on mixing for various salt concentrations. In addition, we have measured the pH both in the complex coacervate and in the dilute phase after complex coacervation was complete. We find that the pH in the dilute phase does change, but remains constant at 6.46 $\pm$ 0.05 during and after complex coacervation. The pH of the complex coacervates with low enough viscosities to allow measurement of the pH (with salt concentrations larger than 1.0 M) was 6.42 $\pm$ 0.05.

Size-exclusion chromatography

We have checked the lengths of the PAA and PDMAEMA polymers using size-exclusion chromatography. Figure 3 shows the chromatogram traces of PAA and PDMAEMA in 10 mM phosphate buffer, pH 6.5.

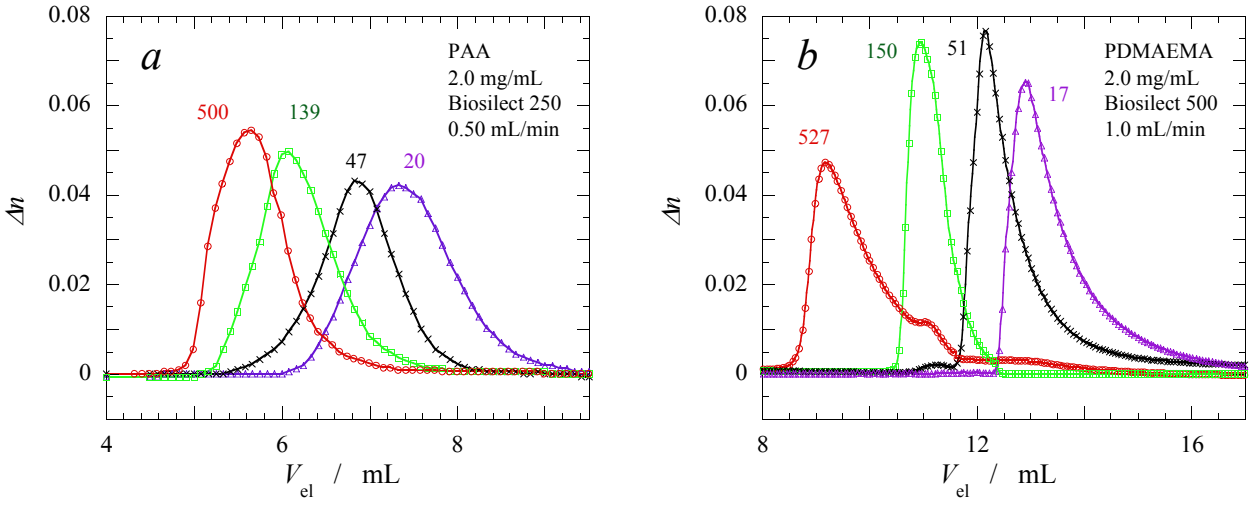

Figure 3: (a) Elution profile of PAA from size-exclusion chromatography for four different chain lengths, measured on a Biosilect-250 column at 2.0 mg/mL in a 10 mM phosphate buffer at pH 6.5 and a flow rate of 0.50 mL/min. At this flow rate, elution peaks are also broadened by diffusion. (b) Elution profile of PDMAEMA from size-exclusion chromatography for four different chain lengths, measured on a Biosilect-500 column at 2.0 mg/mL in a 10 mM phosphate buffer at pH 6.5 and a flow rate of 1.0 mL/min.

Frequency sweeps of uncomplexed polymer solutions

Semidilute solutions of either PAA or PDMAEMA alone show significantly different rheological behavior from the complex coacervates formed when mixing them. Figure 4 shows frequency sweeps of $PDMAEMA_{527}$ and PAA_{500} stock solutions at 0.50 M salt and at the same concentrations as estimated for the complex coacervates.

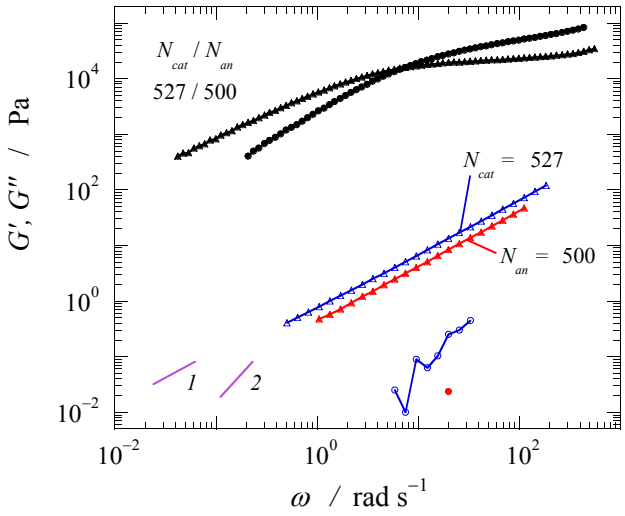

Figure 4: Frequency sweeps of $PDMAEMA_{527}$ and PAA_{500} stock solutions at 250 g/L, compared with a frequency sweep of a $PDMAEMA_{527}$ / PAA_{500} complex coacervate at 0.50 M salt.

Amplitude sweeps

We use amplitude sweeps to establish the extent of the regime of linear viscoelastic response. Figure 5 shows normalized amplitude sweeps for PDMAEMA / PAA complex coacervates with N_{cat} / N_{an} = 527 / 500 at salt concentrations ranging from 0.50 M to 1.1 M. The linear viscoelastic regime extends typically up to 50% strain.

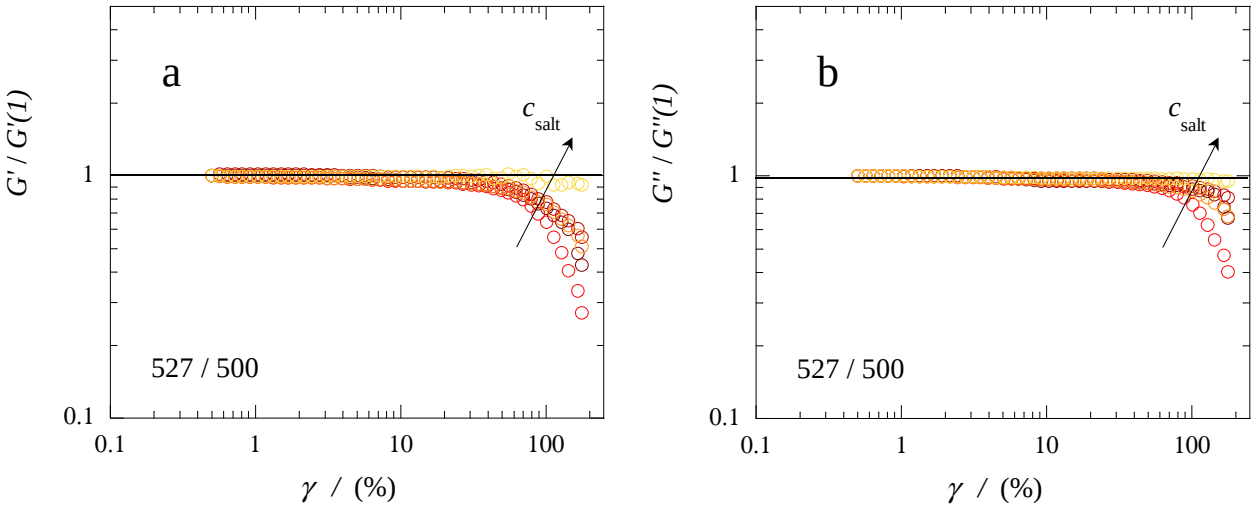

Figure 5: Amplitude sweeps of PDMAEMA / PAA complex coacervates of chain length N_{cat} / N_{an} = 527 / 500 at different salt concentrations (in the direction of the arrow: 0.50, 0.60, 0.75, 0.85 and 1.1 M KCl) at an angular frequency of 1 rad/s. (a) Storage modulus as a function of strain, normalized by the storage modulus at 1% strain. (b) Loss modulus as a function of strain, normalized by the loss modulus at 1% strain.

Effect of solvent evaporation during rheological measurements

We record a frequency sweep at the beginning and at the end of each measurement series to check the efficiency of the solvent blocker we use. Figure 6 shows two typical frequency sweeps for PDMAEMA / PAA complex coacervates with N_{cat} / N_{an} = 527 / 500 at a salt concentration of 0.80 M. The total measurement time between these two frequency sweeps was 4 hours and 20 minutes.

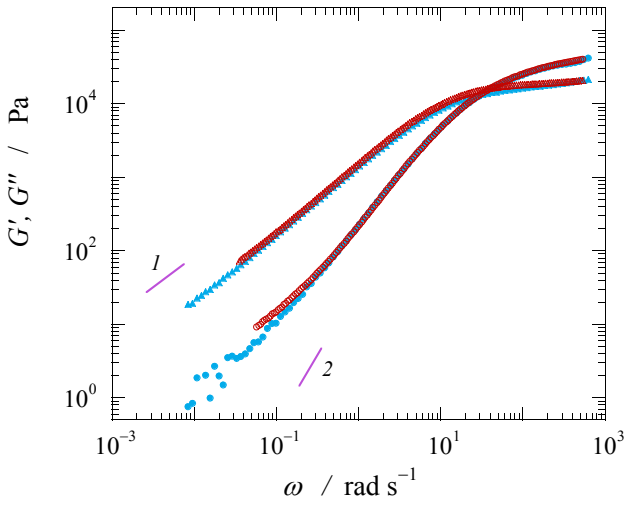

Figure 6: Frequency sweeps of PDMAEMA / PAA complex coacervates of chain length N_{cat} / N_{an} = 527 / 500 at 0.80 M salt and 20 °C. Filled symbols correspond to a frequency sweep recorded at 15 minutes after loading the sample in a CP25 geometry on an Anton Paar MCR501 rheometer with an evaporation blocker. Open symbols correspond to a frequency sweep recorded 4 hours and 35 minutes after loading the sample. The effect of evaporation in this sample at 20 °Cis negligible during our measurement series.

Comparison of step-strain and step-stress measurements

We check that the feedback loop in the stress-controlled rheometer allows carrying out the step-strain measurements with sufficient accuracy on the time scales reported in the main text, by directly converting our step-strain measurements $G(t)$ into creep functions $J(t)$ and vice versa.

Calculation of creep curves from relaxation moduli

To convert experimentally measured relaxation moduli into creep curves, we use the numerical method outlined by Hopkins and Hamming for the convolution integral of the relaxation modulus and creep compliance: [1]

$$\int_0^t \phi(\tau)\psi(t-\tau)\,\mathrm{d}t = 1 \tag{2}$$

where $\psi(t)$ is the normalized relaxation modulus $G(t)/G(0)$ and $\phi(t)$ is the normalized creep compliance $J(t)/J(0)$. In Figure 7b and e we compare the converted creep functions to experimentally measured creep curves. All converted creep curves agree well with the experimentally determined creep compliance curves over the full range of time scales. Only at very short times we sometimes find minor differences between both curves, due to limitations of the feedback loop. The predicted terminal relaxation times and viscosities are identical to the values obtained from the experimentally measured creep compliance curves.

Calculation of relaxation moduli from creep curves

The conversion of creep curves $J(t)$ into relaxation moduli $G(t)$ is numerically much more problematic. The Fourier transform of the compliance is not a convergent integral. The alternative Laplace and inverse Laplace transform can only be calculated for simple analytical formula.[2,3] To overcome this problem, we use a two-step conversion, following the approach outlined by Evans *et al.*[3]

First, we convert the creep compliance into the complex modulus:

$$G^*(\omega) = \frac{i\omega}{i\omega J(0) + \left(1 - e^{-i\omega t_1}\right)\frac{J_1 - J(0)}{t_1} + \frac{e^{-i\omega t_N}}{\eta} + \sum_{k=2}^{N}\left(\frac{J_k - J_{k-1}}{t_k - t_{k-1}}\right)\left(e^{-i\omega t_{k-1}} - e^{-i\omega t_k}\right)} \tag{3}$$

Since even small uncertainties in the creep compliance still give rise to amplifications in the complex modulus, we fitted the compliance data to an empirical function: $J(t) = (t/\eta) + a + b \times \tanh\left(c + d\ln t + e\ln^2 t + f\ln^3 t\right)$.[3] The fit parameters are given in the caption of Figure 7.

Storage and loss moduli can be obtained from the real and imaginary parts of the complex modulus, respectively. In a second step, we calculate the relaxation spectrum from both storage and loss moduli, as outlined in the following section (Equations 8 to 13). Finally, we convert the relaxation spectra into the corresponding relaxation moduli, using the following definition of the continuous relaxation spectrum:[2]

$$G(t) = G_e + \int_{-\infty}^{\infty} H(\tau) e^{-t/\tau}\, \mathrm{d}\ln\tau \tag{4}$$

For the conversions shown in Figure Figure 7, we calculated the relaxation spectra from both storage and loss moduli and used their logarithmic average to calculate the average relaxation modulus $G(t)$.

Figure Figure 7 shows the results of both relaxation moduli converted into creep compliances and vice versa, and the experimentally measured curves.

Based on these results, we conclude that for these complex coacervates, step-strain measurements provide an accurate and direct measurement of the relaxation behavior. However, in the samples at low salt concentration, the converted relaxation modulus decays faster than the experimentally measured modulus. Nevertheless, the key features of these relaxation curves (continuously decreasing function, a regime with constant slope at intermediate times and the terminal relaxation time), as discussed in the main text, are reproduced. We note here that we treat the results for very short time scales ($t < 0.5$ s), obtained in step-strain and step-stress measurements, with caution, because of limitations of the feedback loop. Instead, we use frequency sweeps to access the relaxation behavior of complex coacervates at these short time scales, as explained in the main text.

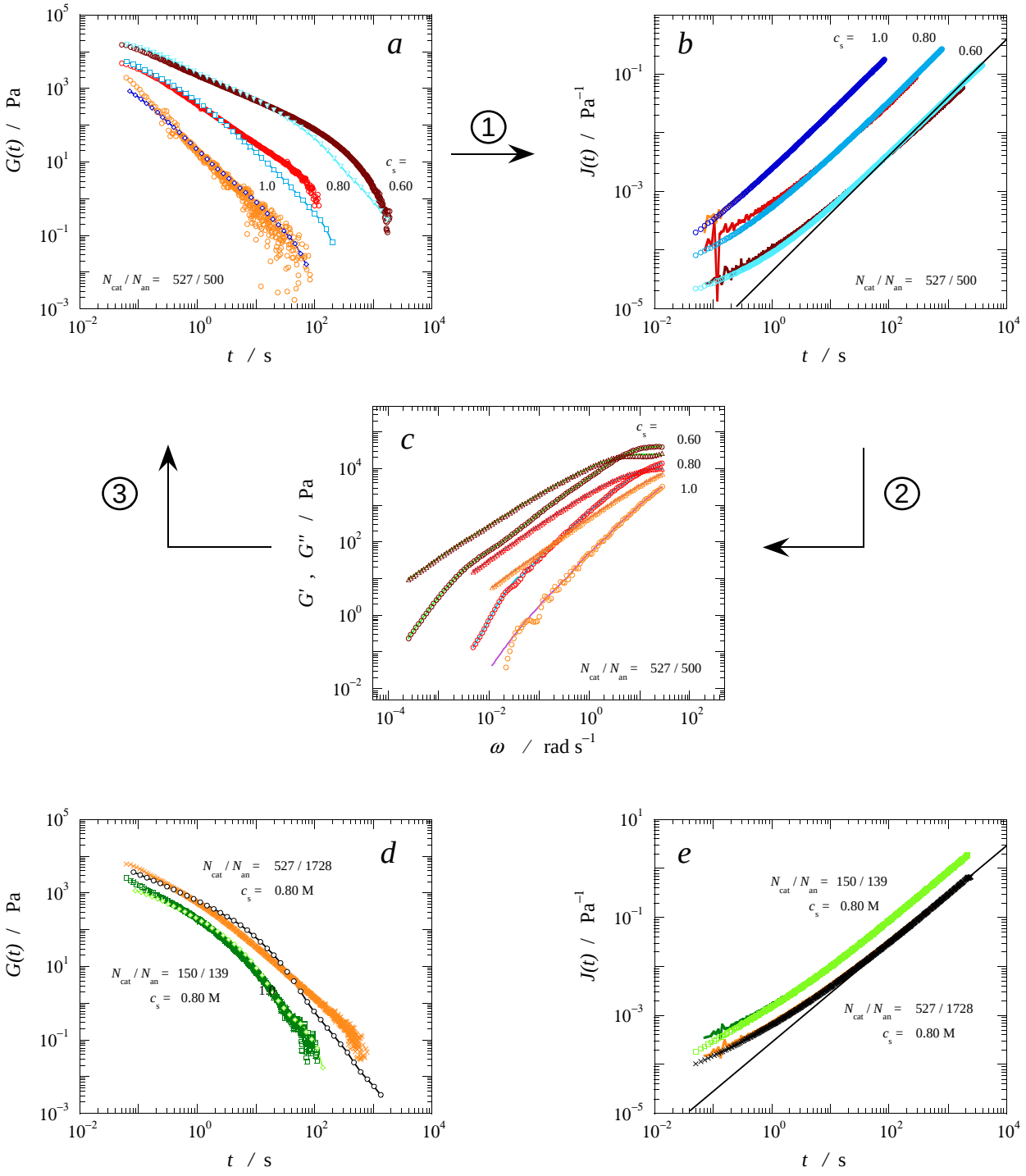
a
b
c
d
e
G(t) / Pa
J(t) / Pa⁻¹
G′ , G″ / Pa
t / s
ω / rad s⁻¹
c_s = 1.0 0.80 0.60
N_cat / N_an = 527 / 500
N_cat / N_an = 527 / 1728
N_cat / N_an = 150 / 139
c_s = 0.80 M
1
2
3

Figure 7: (previous page) (a) Relaxation moduli: measured (circles) and converted from creep compliance measurements (triangles, squares and diamonds); (b) creep compliance curves: measured (circles) and converted from relaxation moduli (lines); (c) storage and loss moduli, which are obtained as an intermediate step in the conversion from creep compliance to relaxation modulus: converted points and smoothed lines; (d) like (a) for different polymer chain lengths; (e) like (b) for different polymer chain lengths. The conversion from relaxation modulus to creep compliance (1) is done, using Equation 2 and the method of Hopkins-Hamming. For the conversion from creep compliance to relaxation modulus we use Equation 3 in step (2) and Equations 8 to 13 and 4 in step (3) . For step (2), we fit the creep compliance data to the empirical function described above, using the following parameters: for the curves in (b), $c_s = 0.60$, $\eta = 3.63\times 10^4$, $a = 1.40\times 10^{-3}$, $b = 1.40\times 10^{-3}$, c = -1.98, d = 0.401, e = -0.0245 and $f = 4.6 \times 10^{-3}$; $c_s = 0.80$, $\eta = 3.08 \times 10^3$, $a = 5.05 \times 10^{-4}$, $b = 7.09 \times 10^{-4}$, c = -0.447, d = 0.158, e = 0.0281 and $f = 2.0 \times 10^{-3}$; $c_s = 1.0$, $\eta = 4.84 \times 10^2$, $a = 1.20 \times 10^{-3}$, $b = 1.40 \times 10^{-3}$, c = -0.681, d = 0.189, e = 0.0237 and $f = 1.1 \times 10^{-3}$; and for the curves in (e), N_{cat}/N_{an} = 527/1728, $c_s = 0.80$, $\eta = 3.45 \times 10^3$, $a = 9.05 \times 10^{-4}$, $b = 8.70 \times 10^{-4}$, c = -0.756, d = 0.308, $e = 6.8 \times 10^{-3}$ and $f = 3.8 \times 10^{-3}$; and N_{cat}/N_{an} = 150/139, $c_s = 0.80$, $\eta = 1.18 \times 10^3$, $a = 6.73 \times 10^{-4}$, $b = 1.30 \times 10^{-3}$, c = -0.0034, d = 0.223, e = 0.0268 and $f = 8.3 \times 10^{-4}$. The labels indicate the chain lengths and salt concentrations. The straight, solid, black lines in (b) and (e) indicate a power law with a slope of 1, representing the long-time viscous limit in the creep curves.

Relaxation time spectra

We calculate relaxation time spectra for the polyelectrolyte complex coacervates by iterative fitting of the relaxation modulus ($G(t)$) and the storage ($G'(\omega)$) and loss modulus ($G''(\omega)$) to a sum of Maxwell elements, each with a discrete relaxation time, according to Baumgaertel and Winter.[4,5]

$$G(t) = \sum_{i=0}^{N} G_i e^{-t/\tau_i} \tag{5}$$

$$G'(\omega) = \sum_{i=0}^{N} \frac{G_i \omega^2 \tau_i^2}{1+\omega^2\tau_i^2}$$

$$G''(\omega) = \sum_{i=0}^{N} \frac{G_i \omega \tau_i}{1+\omega^2\tau_i^2}\,. \tag{6}$$

The N relaxation modes, defined by their relaxation strength G_i and their relaxation time τ_i, are taken equally spaced on a logarithmic scale. The corresponding relaxation time spectrum ($H(\tau)$) of the polyelectrolyte complex is obtained as

$$H(\tau) = \sum_{i=0}^{N} G_i \delta\left(1 - \frac{t}{\tau_i}\right) \tag{7}$$

where $\delta(x)$ denotes the Dirac delta function.

We confirm the fitting procedure of our relaxation time spectra by calculating the relaxation time spectra in an independent procedure from either the storage or the loss moduli using the following approximate interrelations from Williams and Ferry.[2]

For the relaxation time spectrum calculation from the storage modulus, the approximate relation depends on the local negative slope of the relaxation time spectrum on a double logarithmic plot (m). For the regions with a negative slope $m < 1$, the spectrum is given by the product of the storage modulus and its local derivative:

$$H(\tau) = a_1(m)\, G'(\omega) \left. \frac{\mathrm{d}\log G'(\omega)}{\mathrm{d}\log \omega} \right|_{\frac{1}{\omega}=\tau} . \tag{8}$$

The correction factors $a_1(m)$ are defined by

$$a_1(m) = \frac{2-m}{2\Gamma(2-m/2)\Gamma(1+m/2)} = \frac{\sin(m\pi/2)}{m\pi/2} \tag{9}$$

where $\Gamma(x)$ is the Gamma function. For the regions with a negative slope $1 < m < 2$:

$$H(\tau) = a_2(m)\, G'(\omega) \left(2 - \frac{\mathrm{d}\log G'(\omega)}{\mathrm{d}\log \omega} \right) \Bigg|_{\frac{1}{\omega}=\tau} \tag{10}$$

where the correction factors $a_2(m)$ are defined by

$$a_2(m) = \frac{m}{2\Gamma(2-m/2)\Gamma(1+m/2)} = \frac{\sin(m\pi/2)}{\pi(1-m/2)} . \tag{11}$$

Similarly, for the calculation of the relaxation time spectrum from the loss modulus:

$$H(\tau) = b(m)\, G''(\omega) \left(1 - \left| \frac{\mathrm{d}\log G''(\omega)}{\mathrm{d}\log \omega} \right| \right) \Bigg|_{\frac{1}{\omega}=\tau} \tag{12}$$

where the correction factors $b(m)$ are defined by

$$b(m) = \frac{1+|m|}{2\Gamma(3/2-|m|/2)\Gamma(3/2+|m|/2)} = \frac{\sin(\pi(1+|m|)/2)}{\pi(1-|m|)/2} . \tag{13}$$

We calculate approximate relaxation time spectra using the three approaches described above. The calculations according to Equations 8 to 13 are carried out iteratively as well. First, all correction factors $a(m)$ and $b(m)$ are set to unity and $H(\tau)$ is calculated to first approximation. We then calculate the first order corrections from the local derivative of $\log H(\tau)$ v. $\log \tau$. We repeat this step until we find a self-consistent solution for $H(\tau)$.

Figure 8 shows the relaxation time spectra for one sample, calculated in three different ways, as an example. Both the region with constant slope (m = 0.6) and the apparent plateau region is accurately reproduced in all cases. The terminal relaxation time differs only slightly between the three approaches.

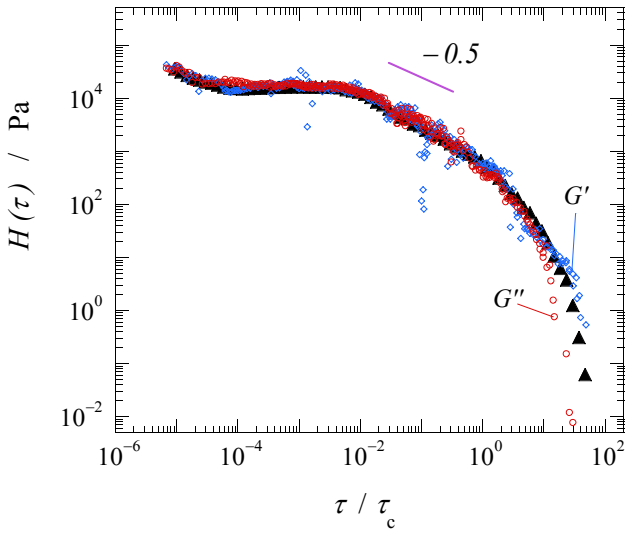

Figure 8: Relaxation time spectrum, corresponding to the frequency sweep master curve, displayed in Fig. 4e in the main text, calculated by fitting both storage and loss modulus to a sum of Maxwell elements (▲), from the storage modulus data (Equations 8 and 9, ◇) and from the loss modulus data (Equations 12 and 13, ○). The shift factors are plotted in Fig. 5 in the main text.

Non-stoichiometric complex coacervates

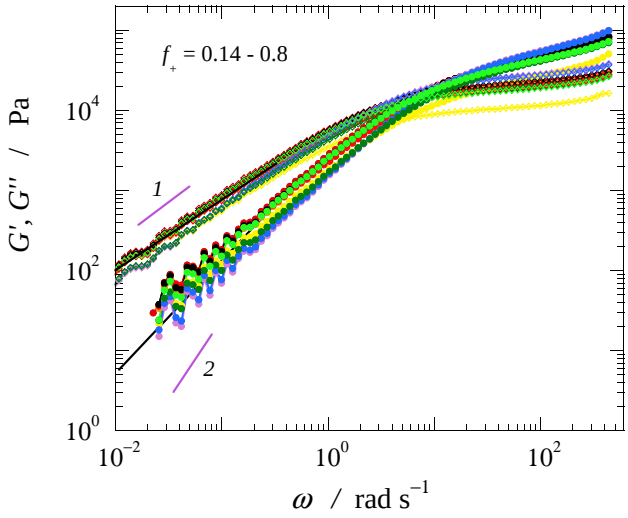

Figure 9: Frequency sweeps of PDMAEMA / PAA complex coacervates of chain length N_{cat} / N_{an} = 527 / 500 at 0.70 M salt at different overall stoichiometry (data for f^+ = 0.19, 0.29, 0.36, 0.45, 0.53, 0.63, 0.71, 0.77, 0.83 and 0.89 are shown).

Key rheological properties of stoichiometric complex coacervates

Table 1: Rheological parameters of stoichiometric complex coacervates.

N_{cat}	N_{an}	f^+	c_{salt} (M)	τ_c (s)	G_c (Pa)	η_0 (Pa s)	τ_R (s)	$G(\tau_R)$ (Pa)
527	1728	0.5	0.60	2.4×10^2	8.1×10^2	1.9×10^5	1.2×10^4	0.98
			0.70	1.2×10^2	6.1×10^2	8.0×10^4	5.0×10^3	0.61
			0.80	47	8.5×10^2	9.0×10^3	5.0×10^2	0.70
			1.0	7.4	1.1×10^3	3.9×10^2	1.3×10^2	0.31
			1.2	0.47	4.0×10^2	52	10	0.21
			1.4			2.3		
527	500	0.5	0.50	1.1×10^2	1.3×10^3	9.5×10^4		
			0.60	20	1.1×10^3	2.0×10^4	1.6×10^3	0.60
			0.70	17	8.0×10^2	5.4×10^3		
			0.80	5.0	6.0×10^2	2.7×10^3	2.0×10^2	0.17
			0.90	2.4	5.5×10^2	6.4×10^2		
			1.0				15	0.059
			1.1	0.25	4.8×10^2	1.1×10^2		
			1.2	0.050	4.5×10^2	12.4		
			1.3			2.4		
150	139	0.5	0.50	10	3.5×10^3	2.8×10^4	5.9×10^2	0.93
			0.60	4.0	2.8×10^3	7.3×10^3		
			0.70	1.4	2.5×10^3	1.2×10^3		
			0.90	0.30	1.5×10^3	4.5×10^2	40	0.29
			1.0	0.17	7.0×10^2	95		
			1.1	0.090	3.3×10^2	9.5		
51	47	0.5	0.27	0.77	9.5×10^3	8.6×10^3		
			0.35	0.51	9.5×10^3	5.0×10^3		
			0.40	0.24	8.7×10^3	1.7×10^3		
			0.50	0.10	9.4×10^3	6.4×10^2	39	0.77
			0.60	0.049	8.0×10^3	3.3×10^2		
			0.70	0.026	6.5×10^3	1.0×10^2	5.0	0.18
			0.80			12		
			0.85			4.3		
17	20	0.5	0.22	0.090	1.4×10^4	1.4×10^3		
			0.40	0.013	1.2×10^4	3.1×10^2	0.79	3.3
			0.50	2.5×10^{-3}	7.0×10^3	90		
			0.58	1.0×10^{-3}	2.4×10^3	9.4		

References

(1) Hopkins, I. L.; Hamming, R. W. *J. Appl. Phys.* **1957**, *28*, 906–909.
(2) Ferry, J. D. *Viscoelastic properties of polymers*; John Wiley & Sons, 1980.
(3) Evans, R. M. L.; Tassieri, M.; Auhl, D.; Waigh, T. A. *Phys. Rev. E* **2009**, *80*, 012501.
(4) Baumgaertel, M.; Winter, H. H. *Rheologica Acta* **1989**, *28*, 511–519.
(5) Baumgaertel, M.; Winter, H. H. *Journal of Non-Newtonian Fluid Mechanics* **1992**, *44*, 15–36.